Multiscale time integration of thermo-mechanically coupled problems with energy-momentum consistent finite element methods in time

Michael Groß

Chair of Applied Mechanics/Dynamics
Chemnitz University of Technology

March 21, 2013

GAMM 2013 – Section S7: Coupled Problems

Multiscale time integration in coupled problems

Felippa & Park [2004], Markovic et al. [2005], Matthies, Niekamp & Steindorf [2006], Kassiotis, Colliat, Ibrahimbegovic & Matthies [2009]

1. Time stepping with different time step sizes is preferred

Finite difference methods (partitioned strategy)

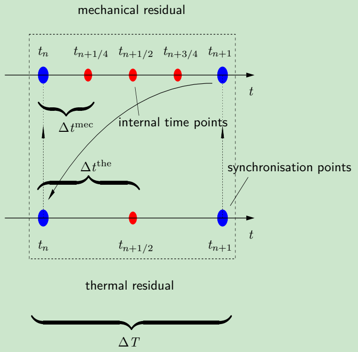

Finite element methods (monolithic strategy)

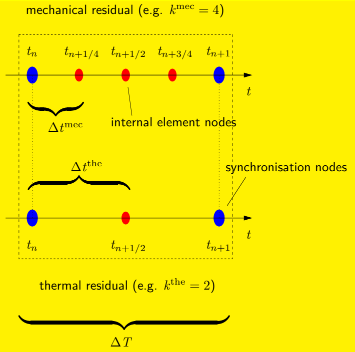

2. Energy consistent time stepping is generally desirable for improving numerical stability

Simulation with different time step sizes

[1] Belytschko & Mullen [1978], Hughes & Liu [1978], Park & Housner [1982], Liu [1983], Smolinski, Belytschko & Neal [1988], Smollinski, Sleith & Belytschko [1996], Smollinski & Wu [1998,2000], Felippa, Park & Farhat [2001], Gravouil & Combescure [2001], Marsden & West [2001], Rugonyi & Bathe [2001], Ibrahimbegovic & Markovic [2003], Romero [2010]

[2] Hughes & Hulbert [1988], Masud & Hughes [1997], Bottasso [2002], Larsson, Hansbo & Runesson [2003], Hübner, Walhorn & Dinkler [2004], Michler, Hulshoff, van Brummelen & de Borst [2004], Hansbo, Hermannsson & Svedberg [2004], Tezduyar, Sathe, Schwaab & Conklin [2008]

Finite difference methods in time[1]

1. Semi-implicit time integration of non-uniform meshes
   - nodal partitioning
   - element partitioning
2. Mixed time integration (field partitioning) of
   - area and boundary coupled problems
   - problems with inelastic media
3. Energy-momentum time integration of coupled problems

Finite element methods in time[2]

1. Space-time Galerkin methods
   - solid mechanics
   - area and boundary coupled field problems
2. Time-discontinuous least squares methods in fluid flow problems
3. Multiple timescale problems
4. NO energy-consistent time integration

Dynamics of solid inelastic isotropic media

Oden [1972], Gurtin [1981], Miehe [1988], Holzapfel [2000], Andrews [2005], Chernyshev [2007], Fernández & Kuttler [2010]

Equation of motion

1. Lagrangian local momentum balance

$$\boldsymbol{v}_t := \frac{\partial \boldsymbol{\varphi}_t}{\partial t} \qquad \boxed{\frac{\partial \boldsymbol{v}_t}{\partial t} \overset{!}{=} \frac{1}{\rho_0}\,\mathrm{DIV}[\boldsymbol{F}_t \boldsymbol{S}_t] + \boldsymbol{b}_t} \qquad \boldsymbol{F}_t := \frac{\partial \boldsymbol{\varphi}_t}{\partial \boldsymbol{X}}$$

2. Total second Piola-Kirchhoff stress tensor

$$\boldsymbol{S}_t := \boldsymbol{S}_t^{\mathrm{ela}} + \boldsymbol{S}_t^{\mathrm{vis}} + \boldsymbol{S}_t^{\mathrm{the}} \qquad \boldsymbol{S}_t^{\mathrm{ela}} := 2\,\frac{\partial \hat{\Psi}_{\mathrm{ela}}(\boldsymbol{C}_t)}{\partial \boldsymbol{C}}$$

Elastic constitutive equations in decoupled form

1. Elastic free energy function

$$\hat{\Psi}_{\mathrm{ela}}(\boldsymbol{C}_t) := \hat{\Psi}_{\mathrm{ela}}^{\mathrm{iso}}(I_t^{\mathbf{C}^{\mathrm{iso}}}, II_t^{\mathbf{C}^{\mathrm{iso}}}) + \hat{\Psi}_{\mathrm{ela}}^{\mathrm{vol}}(III_t^{\mathbf{C}}))$$

2. Right Cauchy-Green stress tensor

$$\boldsymbol{C}_t := \boldsymbol{C}_t^{\mathrm{vol}}\,\boldsymbol{C}_t^{\mathrm{iso}} \qquad \boldsymbol{C}_t^{\mathrm{iso}} := [III_t^{\mathbf{C}}]^{-1/n_{\mathrm{dim}}}\,\boldsymbol{C}_t$$

3. Hyperelastic stress tensor

$$\boldsymbol{S}_t^{\mathrm{ela}} := 2 III_t^{\mathbf{C}}\,\mathrm{D}\hat{\Psi}_{\mathrm{ela}}^{\mathrm{vol}}\,\boldsymbol{C}_t^{-1} + [III_t^{\mathbf{C}}]^{-1/n_{\mathrm{dim}}}\,\mathrm{DEV}_{\mathbf{C}^{\mathrm{iso}}}\left[\boldsymbol{S}_{\mathrm{ela}}^{\mathrm{iso}}(\boldsymbol{C}_t^{\mathrm{iso}})\right]$$

Isotropic finite viscoelasticity

Miehe[1988], Le Tallec et al. [1993], Kaliske [1995], Reese & Govindjee [1998], Reese [2001], Kleuter [2007], Hartmann & Hamkar [2010]

Intermediate configuration

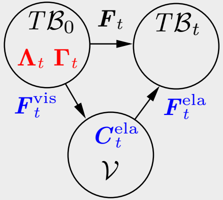

Viscous kinematic equations

1. Viscous internal variable

$$\boldsymbol{\Gamma}_t := [\boldsymbol{F}_t^{\mathrm{vis}}]^T \boldsymbol{F}_t^{\mathrm{vis}}$$

2. 'Elastic' metric tensor

$$\boldsymbol{\Lambda}_t := \boldsymbol{C}_t \boldsymbol{\Gamma}_t^{-1} = \boldsymbol{\Lambda}_t^{\mathrm{vol}} \boldsymbol{\Lambda}_t^{\mathrm{iso}}$$

$$\boldsymbol{\Lambda}_t^{\mathrm{iso}} := [III_t^{\boldsymbol{\Lambda}}]^{-1/n_{\mathrm{dim}}} \boldsymbol{\Lambda}_t$$

Viscous constitutive equations in decoupled form

1. Viscous free energy function

$$\hat{\Psi}_{\mathrm{vis}}(\boldsymbol{\Lambda}_t) := \hat{\Psi}_{\mathrm{vis}}^{\mathrm{iso}}(I_t^{\boldsymbol{\Lambda}^{\mathrm{iso}}}, II_t^{\boldsymbol{\Lambda}^{\mathrm{iso}}}) + \hat{\Psi}_{\mathrm{vis}}^{\mathrm{vol}}(III_t^{\boldsymbol{\Lambda}})$$

2. Viscous Mandel stress tensor and strain rate tensor

$$\boldsymbol{M}_t^{\mathrm{vis}} := \boldsymbol{C}_t \boldsymbol{S}_t^{\mathrm{vis}} = 2\, \boldsymbol{C}_t \frac{\partial \hat{\Psi}_{\mathrm{vis}}(\boldsymbol{\Lambda}_t)}{\partial \boldsymbol{C}} \qquad \boldsymbol{L}_t^{\mathrm{vis}} := \frac{1}{2} [\boldsymbol{\Gamma}_t]^{-1} \frac{\partial \boldsymbol{\Gamma}_t}{\partial t}$$

3. Local evolution equation

$$\boxed{\boldsymbol{M}_t^{\mathrm{vis}} \overset{!}{=} \boldsymbol{Y}_t^{\mathrm{vis}} := n_{\mathrm{dim}}\, V_{\mathrm{sph}}\, \mathrm{SPH}([\boldsymbol{L}_t^{\mathrm{vis}}]^T) + 2\, V_{\mathrm{dev}}\, \mathrm{DEV}([\boldsymbol{L}_t^{\mathrm{vis}}]^T)}$$

Thermodynamics of solids

Oden [1972], Miehe [1988], Holzapfel & Simo [1996], Bérardi et al. [1996], Lion [1997], Reese [2000], Boukamel et al. [2001], Hartmann [2003], Heimes [2005]

Thermal time evolution

1. Lagrangian local entropy balance

$$\boxed{\frac{\partial \eta_t}{\partial t} \overset{!}{=} -\frac{1}{\theta_t}\,\mathrm{DIV}[\boldsymbol{Q}_t] + \frac{D_t^{\mathrm{vis}}}{\theta_t}} \qquad D_t^{\mathrm{vis}} = \boldsymbol{M}_t^{\mathrm{vis}} : \boldsymbol{L}_t^{\mathrm{vis}}$$

2. Total entropy

$$\eta_t := -\frac{\partial \hat{\Psi}_{\mathrm{the}}(\boldsymbol{C}_t, \theta_t)}{\partial \theta} = \eta^{\mathrm{vol}}(III_t^{\mathbf{C}}) + \eta^{\mathrm{cap}}(\theta_t)$$

3. Linear specific heat capacity

$$\theta_t \, \frac{\partial \eta^{\mathrm{cap}}(\theta_t)}{\partial \theta} := c_0\,(1 + c_1 \vartheta_t)$$

Thermal constitutive equations

1. Thermal free energy

$$\hat{\Psi}_{\mathrm{the}}(\boldsymbol{C}_t, \theta_t) := \hat{\Psi}_{\mathrm{the}}^{\mathrm{cap}}(\theta_t) - 2\, n_{\mathrm{dim}}\, \beta\, \vartheta_t \sqrt{III_t^{\mathbf{C}}}\, \mathrm{D}\hat{\Psi}_{\mathrm{ela}}^{\mathrm{vol}}(III_t^{\mathbf{C}})$$

2. Fourierian isotropic heat conduction law

$$\boldsymbol{Q}_t := -k_0\, \boldsymbol{C}^{-1} \mathrm{GRAD}[\theta_t] \qquad k_0 := k\, J^{\mathrm{the}}(\theta_t) = k\, e^{n_{\mathrm{dim}}\, \beta\, \vartheta_t}$$

Galerkin finite element approximation

[1] G. [2004], G., Betsch & Steinmann [2004], G. [2009], G. & Betsch [2010], G. & Betsch [2011]

[2] Simo et al. [1992], Galvanetto & Crisfield [1996], Gonzales [2000], Betsch & Steinmann [2000,2001,2002], Brank [2002], Sansour et al. [2004], Armero & Romero [2001a,b], Ibrahimbegovic & Mamouri [2002], Meng & Laurson [2002], Noels et al. [2006], Armero [2006,2007,2008], Hesch [2007], Romero [2009,2010a,b], Hesch & Betsch [2011]

Galerkin space-time approximation[1]

1. Standard continuous finite elements in space for $\mathcal{B}_0$
2. Standard continuous time finite elements for $\boldsymbol{\varphi}_t$, $\boldsymbol{v}_t$
3. Modified discontinuous time finite elements for θ_t

Non-standard constitutive approximations in time

1. Nodal approximations of strain and entropy

$$\boldsymbol{C}^{\mathrm{mec},*}_{\xi_K} := \sum_{I=1}^{m_{\mathrm{mec}}} M_I^{\mathrm{mec}}(\xi_K)\, \boldsymbol{C}^*_{t_I} \qquad \eta^*_{\zeta_L} := \sum_{J=1}^{m_{\mathrm{the}}} M_J^{\mathrm{the}}(\zeta_L)\, \eta^*_{t_J}$$

2. Algorithmic stress and local entropy production

$$\boldsymbol{S}^*_{\xi_K} := \boldsymbol{S}_{\xi_K} + \boldsymbol{S}^{\mathrm{alg}}_{\xi_K} \quad \text{in the equation of motion}$$

$$D^{\mathrm{int},*}_{\zeta_L} := D^{\mathrm{int}}_{\zeta_L} + D^{\mathrm{alg}}_{\zeta_L} \quad \text{in the entropy balance equation}$$

Beneficial effects

1. As stable as energy-momentum finite difference schemes[2], and
2. As accurate as higher order Galerkin methods in time[1]

Galerkin-based energy consistency

French & Schaeffer [1990], Betsch & Steinmann [2000,2001], Larson & Niklasson [2001], Hansbo [2001], Betsch & Steinmann [2002], Cockburn [2003], G. [2004], G., Betsch & Steinmann [2005], Bui [2007], Mohr, Menzel & Steinmann [2008], Bargmann [2008], G. [2009], G. & Betsch [2010,2011]

Balance of relative total energy

$$\frac{\mathrm{d}\mathcal{H}(t)}{\mathrm{d}t} = \int_{\mathscr{B}_0} \frac{\theta_\infty}{\theta_t} D_t^{\text{tot}} \leqslant 0 \qquad \mathcal{H}(t) = \int_{\mathscr{B}_0} \rho_0 \boldsymbol{v}_t \cdot \boldsymbol{v}_t + \psi_t + (\theta_t - \theta_\infty)\,\eta_t$$

Algorithmic balance of relative total energy

$$\begin{aligned}
\mathcal{H}(T) - \mathcal{H}(t_0) &= \int_{\mathscr{T}}\int_{\mathscr{B}_0} \rho_0 \boldsymbol{v}_t \cdot \frac{\partial \boldsymbol{v}_t}{\partial t} + \int_{\mathscr{T}}\int_{\mathscr{B}_0} \rho_0 \frac{\partial \boldsymbol{v}_t}{\partial t} \cdot \left[\frac{\partial \boldsymbol{\varphi}_t}{\partial t} - \boldsymbol{v}_t\right] \\
&+ \int_{\mathscr{T}}\int_{\mathscr{B}_0} \frac{\partial \Psi_t}{\partial \boldsymbol{F}} : \frac{\partial \boldsymbol{F}_t}{\partial t} - \int_{\mathscr{T}}\int_{\mathscr{B}_0} \frac{\partial \boldsymbol{\varphi}_t}{\partial t} \cdot \left[\rho_0 \frac{\partial \boldsymbol{v}_t}{\partial t} - \mathrm{DIV}[\boldsymbol{F}_t \overline{\boldsymbol{S}}_t]\right] \\
&+ \int_{\mathscr{T}}\int_{\mathscr{B}_0} \frac{\partial \Psi_t}{\partial \boldsymbol{\Gamma}} : \frac{\partial \boldsymbol{\Gamma}_t}{\partial t} + \int_{\mathscr{T}}\int_{\mathscr{B}_0} \frac{\partial \boldsymbol{\Gamma}}{\partial t} : \left[\frac{1}{2}\boldsymbol{\Gamma}_t^{-1} \boldsymbol{M}_t^{\text{vis}} - \boldsymbol{Y}_t^{\text{vis}}\right] \\
&+ \int_{\mathscr{T}}\int_{\mathscr{B}_0} (\theta_t - \theta_\infty) \frac{\partial \overline{\eta}_t}{\partial t} - \int_{\mathscr{T}}\int_{\mathscr{B}_0} (\theta_t - \theta_\infty) \left[\frac{\partial \overline{\eta}_t}{\partial t} + \frac{1}{\theta_t} \mathrm{DIV}[\boldsymbol{Q}_t] - \frac{\overline{D}_t^{\text{int}}}{\theta_t}\right] \\
&\underbrace{\begin{aligned}&+ \int_{\mathscr{T}}\int_{\mathscr{B}_0} \frac{\partial \theta_t}{\partial t} \left[\frac{\partial \Psi_t^{\text{the}}}{\partial \theta_t} + \overline{\eta}_t\right] \\
&- \int_{\mathscr{T}}\int_{\mathscr{B}_0} \frac{\partial \boldsymbol{F}_t}{\partial t} : \left[\frac{\partial \Psi_t}{\partial \boldsymbol{F}_t} - \boldsymbol{F}_t \overline{\boldsymbol{S}}_t\right]\end{aligned}}_{0} \\
&= -\int_{\mathscr{T}}\int_{\mathscr{B}_0} \frac{\theta_\infty}{\theta_t} D_t^{\text{tot}} \leqslant 0
\end{aligned}$$

Energy consistent time discretisation

Blue brackets have to vanish locally or at least in a weak sence

Multiscale time approximation of the entropy

Entropy approximation at the thermal nodes

$$\eta^*_{\zeta_L} := \sum_{J=1}^{m_{\text{the}}} M_J^{\text{the}}(\zeta_L)\, \eta^*_{t_J} \qquad \eta^*_{t_J} \neq -\frac{\partial \psi(\theta_{t_J}, \boldsymbol{C}^{\text{mec}}_{t_K})}{\partial \theta}$$

Discrete C-projection in time ('Hamiltonian ehG method')

$$\overline{\boldsymbol{C}}^{\text{mec}}_{\zeta_L} \equiv \sum_{I=1}^{m_{\text{mec}}} M_I^{\text{mec}}(\zeta_L)\, \boldsymbol{C}_{t_I} \overset{!}{=} \sum_{J=1}^{m_{\text{the}}} M_J^{\text{the}}(\zeta_L)\, \boldsymbol{C}^*_{t_J} =: \overline{\boldsymbol{C}}^{\text{the}}_{\zeta_L}$$

Discrete η-projection in time ('Projected ehG method')

$$\sum_{K=1}^{m_{\text{the}}} \frac{\partial \theta_{\zeta_L}}{\partial t} \left[\frac{\partial \hat{\Psi}_{\text{the}}(\overline{\boldsymbol{C}}^{\text{mec}}_{\zeta_L}, \theta_{\zeta_L})}{\partial \theta} + \eta^*_{\zeta_L} \right] w_K \overset{!}{=} 0$$

Discrete matrix form

$$\begin{bmatrix} \boldsymbol{C}^*_{t_1} \\ \vdots \\ \boldsymbol{C}^*_{t_{M_{\text{the}}}} \end{bmatrix} := \boldsymbol{W} \otimes \boldsymbol{I} \begin{bmatrix} \boldsymbol{C}_{t_1} \\ \vdots \\ \boldsymbol{C}_{t_{M_{\text{mec}}}} \end{bmatrix}$$

Discrete matrix form

$$\begin{bmatrix} \eta^*_{t_1} \\ \vdots \\ \eta^*_{t_{M_{\text{the}}}} \end{bmatrix} := \boldsymbol{W} \begin{bmatrix} -\partial_\theta \Psi_{\tau_1} \\ \vdots \\ -\partial_\theta \Psi_{\tau_{M_{\text{the}}}} \end{bmatrix}$$

Toy problem of a flying square

Constitutive functions

(in coupled form)

$$\hat{\Psi}^{\text{iso}}(\boldsymbol{A}) := \frac{\mu}{2}\left(I_{\mathbf{A}} - I_{\mathbf{I}} - 2\,\ln III_{\mathbf{A}}^{1/2}\right)$$

$$\hat{\Psi}^{\text{vol}}(\boldsymbol{A}) := \frac{\lambda}{2}\left(\ln^2 III_{\mathbf{A}}^{1/2} + (III_{\mathbf{A}}^{1/2} - 1)^2\right)$$

Simo & Taylor [1982]

Example parameter

Height	h	$1\,\text{cm}$
Width	b	$1\,\text{cm}$
Thermoviscoelastic material due to Simo & Taylor		
Mass density	ρ_0	$8.93\,\text{kg/cm}^2$
First Lamé constant	μ	$7.5\,\text{J/cm}^2$
Second Lamé constant	λ	$30\,\text{J/cm}^2$
Deviatoric viscosity	V_{dev}	$10\,\text{kJs/cm}^2$
Spherical viscosity	V_{sph}	$50\,\text{kJs/cm}^2$
Specific heat capacity	c_0	$0.1\,\text{kJ/cm}^2\text{K}$
	c_1	0
Heat expansion coefficient	β	$10^{-4}\,\text{K}^{-1}$
Heat conduction coefficient	k_0	$0.01\,\text{kW/K}$
Ambient temperature	Θ_∞	$298.15\,\text{K}$
Global iteration tolerance	tol	$10^{-6}\,\text{J}$
Local iteration tolerance	tolevo	$10^{-10}\,\text{J/cm}^2$
Maximum number of iterations	maxit	10
Number of spatial elements	n_{el}	4
Number of spatial nodes	n_{no}	9

Current configurations

($k^{\text{mec}} = k^{\text{the}} = k^{\text{vis}} = 4$, ehG method with entropy projection)

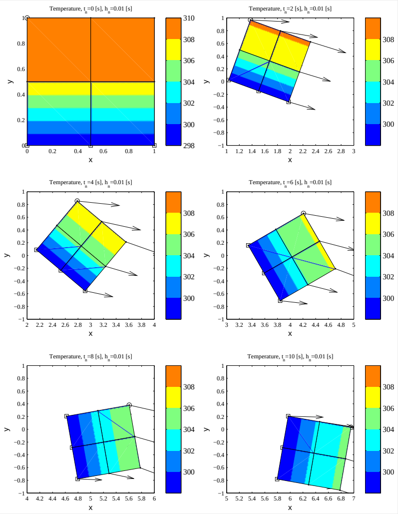

Relative L_2-error of the flying square

Theoretical knowledge

Accuracy order $2k$	for $\boldsymbol{q}$, $\boldsymbol{v}$	alone
Accuracy order $2k$	for $\boldsymbol{\Gamma}$	alone
Accuracy order $2k+1$	for θ	alone

$\rightsquigarrow$ Accuracy order $\min(2k, 2k+1, 2k) = 2k$ for fully coupled problem

Right Cauchy-Green projection (blue lines)

1. coincides with the ehG method
2. preserve the expected accuracy orders $2k$ for each degree k
3. the reference solution is reached increasingly early with increasing degree k.
4. CPU time is more and more saved with increasing degree k.

Entropy projection (red lines)

1. same behaviour as above
2. with exception of a lower order for $k = 2$ in $\boldsymbol{q}$, $\boldsymbol{v}$ and $\boldsymbol{\Gamma}$

L_2-error plots

($k^{\text{mec}} = k^{\text{the}} = k^{\text{vis}} = k$, ehG method with projection)

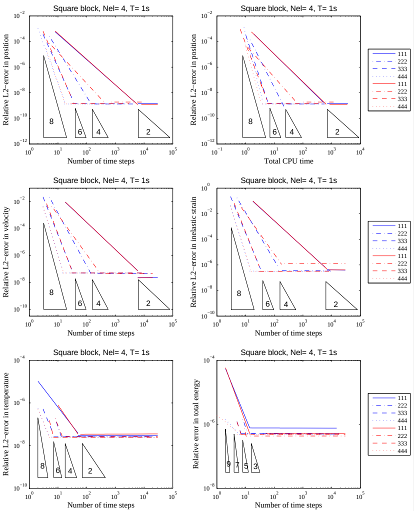

Relative L_2-error of the flying square

Theoretical knowledge

Accuracy order $2k$	for $\boldsymbol{q}$, $\boldsymbol{v}$	alone
Accuracy order $2k$	for $\boldsymbol{\Gamma}$	alone
Accuracy order $2k+3$	for θ	alone

$\rightsquigarrow$ Accuracy order

$$\min(2k, 2k+3, 2k) = 2k$$

for fully coupled problem

Right Cauchy-Green projection (blue lines)

1. preserve the expected accuracy orders $2k$ for each degree k

Entropy projection (red lines)

1. same behaviour as above
2. also for quadratic polynomials

L_2-error plots

($k^{\mathrm{mec}} = k^{\mathrm{the}} - 1 = k^{\mathrm{vis}} = k$, ehG method with projection)

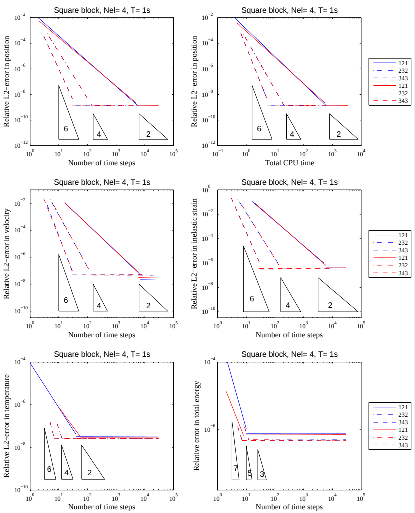

Relative L_2-error of the flying square

Theoretical knowledge

Accuracy order $2k+2$ for $\boldsymbol{q}$, $\boldsymbol{v}$ alone
Accuracy order $2k+2$ for $\boldsymbol{\Gamma}$ alone
Accuracy order $2k+1$ for θ alone

$\rightsquigarrow$ Accuracy order
$\min(2k+2, 2k+1, 2k+2) = 2k+1$
for fully coupled problem

Right Cauchy-Green projection (blue lines)

1. preserve the expected accuracy orders $2k+1$ with exception for quadratic polynomials

Entropy projection (red lines)

1. same behaviour as above

L_2-error plots

($k^{\text{mec}} - 1 = k^{\text{the}} = k^{\text{vis}} - 1 = k$, ehG method with projection)

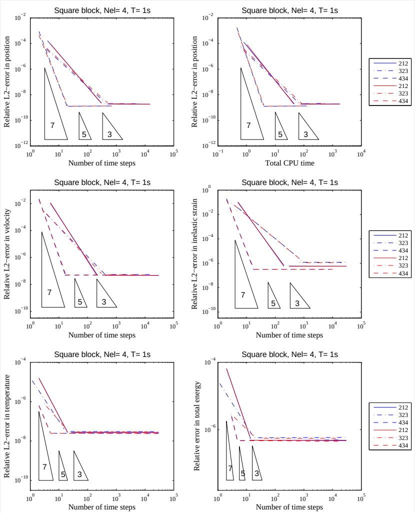

Free flying ring with thermal Dirichlet boundary

Constitutive functions

in decoupled form

$$\hat{\Psi}^{\text{iso}}(\boldsymbol{A}^{\text{iso}}) := \mu_{10}(I_{\mathbf{A}^{\text{iso}}} - I_{\mathbf{I}}) + \mu_{20}(I_{\mathbf{A}^{\text{iso}}} - I_{\mathbf{I}})^2 + \mu_{30}(I_{\mathbf{A}^{\text{iso}}} - I_{\mathbf{I}})^3 + \mu_{01}(II_{\mathbf{A}^{\text{iso}}} - II_{\mathbf{I}}) + \frac{Y_1}{Y_2}\left[1 - e^{-Y_2(I_{\mathbf{A}^{\text{iso}}} - I_{\mathbf{I}})}\right]$$

$$\hat{\Psi}^{\text{vol}}(\boldsymbol{A}) := \frac{\kappa}{50}\left(III_{\mathbf{A}}^{5/2} + III_{\mathbf{A}}^{-5/2} - 2\right)$$

Yeoh [1993], Hartmann & Neff [2003], Heimes [2005]

Example parameter

Inner radius	R_i	5 cm
Outer radius	R_a	15 cm
Thermoviscoelastic material model according to Heimes		
Mass density	ρ_0	112 g/cm^2
Shear moduli	μ_{10}	2500 N/cm
	μ_{20}	210 N/cm
	μ_{30}	0 N/cm
	μ_{01}	0 N/cm
Bulk modulus	κ	10000 N/cm
First Yeoh constant	Y_1	1631 N/cm
Second Yeoh constant	Y_2	0.6
Deviatoric viscosity	V_{dev}	10000 Js/cm^2
Spherical viscosity	V_{sph}	50000 Js/cm^2
Specific heat capacity	c_0	1539 J/cm^{2}K
	c_1	0.00375
Heat expansion coefficient	β	$2.06 \cdot 10^{-4}$ K^{-1}
Heat conduction coefficient	k_0	0.2595 W/K
Ambient temperature	Θ_∞	298.15 K
Global iteration tolerance	tol	10^{-6} J
Local iteration tolerance	tolevo	10^{-9} J/cm^2
Maximum number of iterations	maxit	15
Number of spatial elements	n_{el}	416
Number of spatial nodes	n_{no}	448

Nodal solutions

($k^{\text{mec}} = 1$; $k^{\text{the}} = 4$; $k^{\text{vis}} = 1$; ehG method with entropy projection)

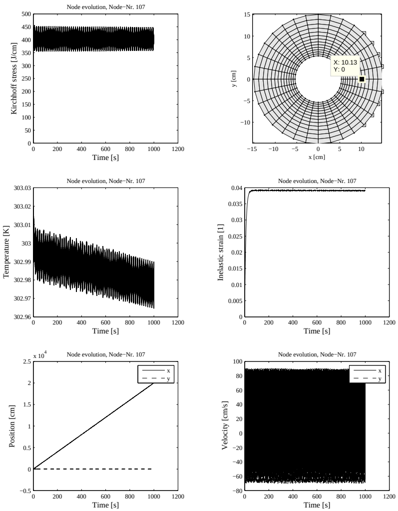

Free flying ring with thermal Dirichlet boundary

Mean time behaviour

1. Constant total linear momentum without external forces
2. Constant total angular momentum without external torques
3. Non-negative viscous and total dissipation
4. Steady decreasing relative total energy

Local behaviour

1. High-frequency solutions leads to high-frequency time evolutions of dissipation, kinetic energy and internal energy
2. But smooth relative total energy and momenta

Physical structure

($k^{\mathrm{mec}} = 1; k^{\mathrm{the}} = 4; k^{\mathrm{vis}} = 1$; ehG method with entropy projection)

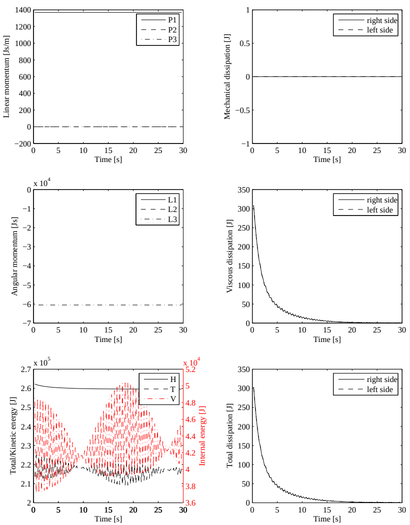

Free flying ring with thermal Dirichlet boundary

Mean time behaviour

1. Stable convergence in the global residuals
2. Stable convergence in the local (viscous) residual
3. Stable iteration number and cpu time per time step

Local behaviour

1. High initial global residuals and slow initial convergence through large time step size
2. But a fast convergence from a moderate residual norm

Convergence behaviour

($k^{\mathrm{mec}} = 1$; $k^{\mathrm{the}} = 4$; $k^{\mathrm{vis}} = 1$; ehG method with entropy projection)

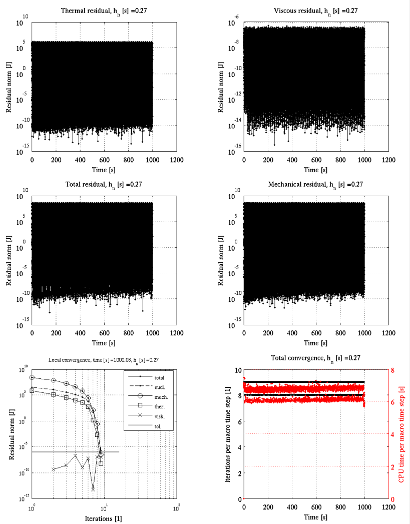

Free flying ring with thermal Dirichlet boundary

Convergence comparison

($k^{\text{mec}} = 1; k^{\text{the}} = 1, \ldots, 4; k^{\text{vis}} = 1, \ldots, 4$; ehG method)

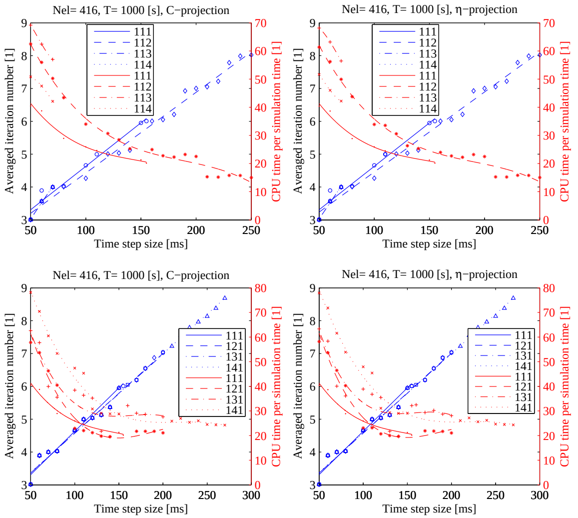

Free flying ring with thermal Dirichlet boundary

Convergence comparison

($k^{\mathrm{mec}} = 2; k^{\mathrm{the}} = 1, \dots, 4; k^{\mathrm{vis}} = 1, \dots, 4$; ehG method)

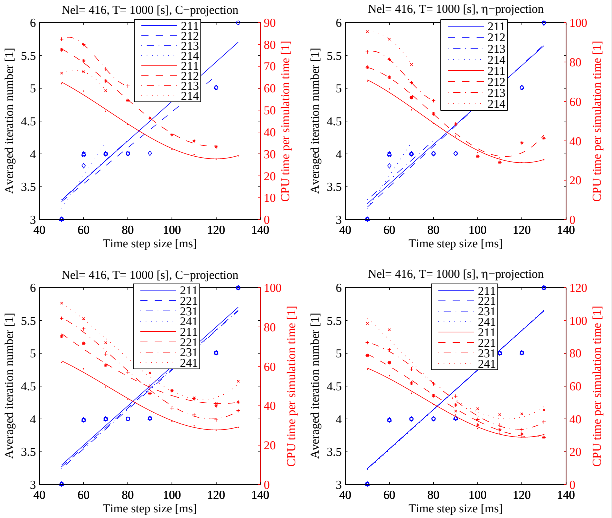

Conclusion

[1]Ibrahimbegovic, Chorfi & Gharzeddine [2001], Hartmann, Quint & Arnold [2008], Birken et al. [2010], Gleim & Kuhl [2013]

1. Goal: A stable Galerkin-based time integration method
   - takes into account different time scales
   - despite of a monolithic solution strategy
2. Algorithmic basis: The ehG method
   - energy-momentum consistent
   - higher-order accurate
   - more stable as standard methods
3. Algorithmic upgrade for the multiscale time integration:
   - entropy approximation projection in two ways
   - $\boldsymbol{C}$-projection includes the original ehG(k) method
4. Results: Multiscale time integration (ehG($k_{\mathrm{mec}}, k_{\mathrm{the}}, k_{\mathrm{vis}}$))
   - both projections show here comparable accuracy and stability
   - mixed time finite elements improve the numerical stability
5. Outlook: A stable (p-)adaptive time integration method [1]